FUDMA Journal of Sciences (FJS)
ISSN online: 2616-1370
ISSN print: 2645 - 2944
Vol. 10 No. 21, November, 2026, pp 318 – 330
DOI: https://doi.org/10.33003/fjs-2026-1021-5720

Comparative Analysis of Microstrip Patch Antenna Using Different Geometrical Shapes at Millimeter Wave Frequency for 5g and Future Wireless Communication Systems

[1]Mohammed Inuwa Usman, [1]Mutari Hajara Ali and [2]Omoleye T Olabode

[1]Department of Physics, Bayero University, Kano State, Nigeria.
[2]Department of Physics, Federal University of Technology, Akure Ondo State Nigeria.

*Corresponding authors' email: miu2000037.mpy@buk.edu.ng

Received: 10 Aug. 2026
Accepted: 17 Sept. 2026
Published: 05 Oct. 2026

ABSTRACT
Microstrip patch antennas are attractive for fifth-generation (5G) wireless communication because they are low-profile, lightweight, and easy to fabricate, but their inherent narrow bandwidth and low efficiency limit their effectiveness at millimeter-wave frequencies. This study presents a comparative analysis of six microstrip patch antenna geometries — rectangular, circular, triangular, square, trapezoidal, and annular ring — designed for 24 GHz on a Fire-Resistant Epoxy 4 (FR4) substrate and simulated in High Frequency Structure Simulator (HFSS). Performance was evaluated in terms of resonant frequency, bandwidth, gain, directivity, return loss (S11), and voltage standing wave ratio (VSWR). All antennas resonated within 3% of the 24 GHz target (24.00–24.725 GHz). The rectangular patch achieved the widest −10 dB bandwidth (3.87 GHz, 15.94%) with a return loss of −28.16 dB and a VSWR of 1.08. The square patch gave the deepest return loss (−29.21 dB) and the lowest VSWR (1.07), while the annular ring patch recorded the highest gain (7.18 dBi) and directivity (8.01 dBi, equal to the square patch). The trapezoidal patch had the narrowest bandwidth (1.00 GHz, 4.17%), and the triangular patch showed the weakest overall performance, with the lowest gain (4.13 dBi) and directivity (5.22 dBi) and the shallowest return loss (−11.02 dB). These results demonstrate that geometric shape selection significantly influences patch antenna performance at millimeter-wave frequencies: the rectangular shape is best for bandwidth, the square for impedance matching, and the annular ring for gain. These findings guide the design of compact, high-performing antennas for 5G and future wireless systems.

Keywords: Microstrip Patch Antenna, Millimeter-Wave, 5G, HFSS, Geometric Shape Comparison

INTRODUCTION

Antennas are metallic devices used for radiating and receiving radio waves, with transmission lines such as waveguides or coaxial cables used to convey electromagnetic energy between a source and an antenna, or between an antenna and a receiver (Balanis, 2016). Several antenna types exist, including wire antennas, microstrip antennas, aperture antennas, array antennas, reflector antennas, and lens antennas, each suited to different application requirements. Among these, microstrip patch antennas have become increasingly attractive for modern wireless systems because of their low profile, light weight, and compatibility with printed-circuit fabrication techniques (Bansal & Gupta, 2020). The emergence of fifth-generation (5G) wireless networks has further intensified interest in this antenna class, as 5G is expected to deliver data rates up to a hundred times those of fourth-generation systems by exploiting millimeter-wave (mm-wave) frequency bands (Agiwal, Roy, & Saxena, 2016; Andrews et al., 2014). This shift toward higher frequencies and higher capacity has created new demands on antenna design, particularly the need for compact radiating elements capable of efficient operation at mm-wave frequencies. Structurally, a microstrip patch antenna consists of a radiating metallic patch printed on a dielectric substrate backed by a ground plane; electromagnetic waves fringe from the edges of the patch into the substrate, reflect off the ground plane, and radiate into free space (Kiruthika &Shanmuganantham, 2016). Microstrip antennas are mechanically durable, well suited to microwave monolithic integrated circuit (MMIC) design, and highly adaptable in terms of resonant frequency, polarization, and radiation pattern depending on the patch shape selected (Bansal & Gupta, 2020). These qualities have made them widely used in space systems, missile systems, and telecommunication applications where low weight, compact size, and low profile are essential (Balanis, 2016; Pandey, Agrawal, & Agrawal, 2019). However, microstrip antennas also suffer from notable operational limitations, including low efficiency, poor polarization purity, a high quality factor, low power-handling capability, and — most critically for high-frequency applications — a very narrow impedance bandwidth (Balanis, 2016; Pandey et al., 2019).

The rapid evolution of wireless communication technology, from first-generation (1G) through fourth-generation Long-Term Evolution (4G/LTE) systems to the emerging 5G standard, has been accompanied at each stage by changes in the bandwidth requirements of compatible devices (Lan, 2023). The transition to 5G, in particular, requires antennas capable of operating efficiently across wider bandwidths and at significantly higher frequencies than earlier generations demanded. This poses a direct challenge for microstrip patch antennas, whose principal limitation — narrow bandwidth — is precisely the characteristic that 5G mm-wave operation stresses most. Because bandwidth, gain, directivity, return loss, and impedance matching are all strongly influenced by the geometry of the radiating patch, the choice of patch shape becomes a critical design variable rather than an incidental one. Yet, despite this sensitivity, many existing microstrip antenna designs for 5G continue to be developed around a single geometry without a systematic, side-by-side

comparison of how alternative shapes perform under identical design and simulation conditions. This leaves antenna designers with limited practical guidance on which geometry offers the best trade-off among competing performance parameters for mm-wave 5G applications — a gap this study seeks to address.

Several studies have attempted to address microstrip antenna performance limitations at mm-wave frequencies, but most have examined only a single shape or a narrow set of shapes. Gemeda, Fante, Goshu, and Goshu (2021) designed a 28 GHz rectangular microstrip patch antenna on FR-4 substrate, simulated in CST, and reported a gain of 7.587 dBi, directivity of 7.509 dBi, radiation efficiency of 98.214%, and a bandwidth of 1.046 GHz, demonstrating competitive performance relative to earlier designs but without exploring alternative geometries. Kiran, Mounisha, Mythily, Akhil, and Kumar (2018) designed a miniaturized rectangular patch antenna on Rogers RT 5880 substrate for 5G, achieving a gain of 2.6 dB and return losses of 21 dB and 31 dB at 28.3 GHz and 50.3 GHz respectively, again restricting the investigation to a single shape. A more directly comparative effort was undertaken by Colaco and Lohani (2020), who evaluated circular, rectangular, and square patch antennas at 27 GHz on RT/Duroid substrate and found the rectangular shape to offer the best bandwidth and gain among the three; however, their comparison was limited to only three geometries and did not include shapes such as the annular ring, trapezium, or triangular patch. Other approaches to improving microstrip antenna performance, including substrate optimization, the addition of parasitic elements, and array configurations, have also been explored in the literature (Bansal & Gupta, 2020). Collectively, these studies confirm that patch geometry meaningfully affects antenna performance, but none provides a broad, consistent comparison across a wide range of shapes — rectangular, circular, triangular, square, trapezoidal, and annular ring — under a single substrate, frequency, and simulation environment, which limits the practical guidance available to designers selecting a geometry for 5G mm-wave applications.

This paper addresses this gap by presenting a comparative analysis of six microstrip patch antenna geometries — rectangular, circular, triangular, square, trapezoidal, and annular ring — designed and simulated at a common mm-wave frequency of 24 GHz using Fire-Resistant Epoxy 4 (FR4) as the substrate material. Unlike prior studies that examine a single shape or a limited subset of shapes, this work evaluates all six geometries under identical design and simulation conditions in High Frequency Structure Simulator (HFSS), assessing performance across five key parameters — bandwidth, gain, directivity, return loss (S11), and voltage standing wave ratio (VSWR) — to identify the shape or shapes offering the best overall performance for 5G and future mm-wave wireless communication systems.

MATERIALS AND METHODS

Six microstrip patch antenna geometries — rectangular, square, circular, triangular, trapezoidal, and annular ring — were designed analytically and subsequently modeled and simulated in High Frequency Structure Simulator (HFSS) software. Each antenna was designed to resonate at a millimeter-wave frequency of 24 GHz on a Fire-Resistant Epoxy 4 (FR4) substrate of relative permittivity εr = 4.4 and thickness h = 1.6 mm. For each geometry, the physical dimensions of the radiating patch were first computed analytically using standard microstrip antenna design equations; the resulting dimensions were then used to construct the corresponding three-dimensional model in HFSS, which was excited with a microstrip line feed and simulated to obtain the bandwidth, gain, directivity, return loss (S11), and voltage standing wave ratio (VSWR) of each design. The general structure of a microstrip patch antenna — comprising a radiating metallic patch, a dielectric substrate, a ground plane, and a microstrip feed line — is shown in Figure 1.

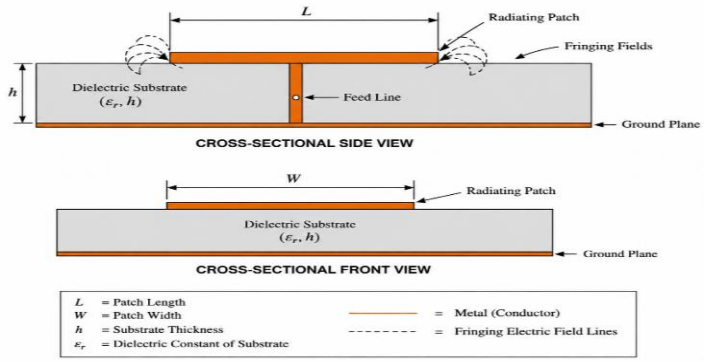


Figure 1: Cross-Sectional Structure of a Microstrip Patch Antenna

Design Procedure

The design procedure for each geometry followed three stages: (i) analytical computation of the patch dimensions from closed-form microstrip antenna design equations, using the target resonant frequency (24 GHz), the substrate dielectric constant, and the substrate height as inputs; (ii) three-dimensional modeling of the resulting patch, substrate, ground plane, and microstrip feed line in HFSS; and (iii) full-wave electromagnetic simulation to extract the bandwidth, gain, directivity, return loss, and VSWR of each design. The six geometries investigated are shown in Figure 2.

In all models, the feed is a microstrip line joined directly to the patch edge; no inset feed or additional matching section was used. An open region (radiation boundary) was created around each model in HFSS, with the solution frequency set to the operating frequency of 24 GHz. Adaptive meshing was run for a maximum of 20 passes with a maximum delta S of 0.02. The frequency sweep range was selected individually for each geometry and therefore differs from one shape to another (Table 2).

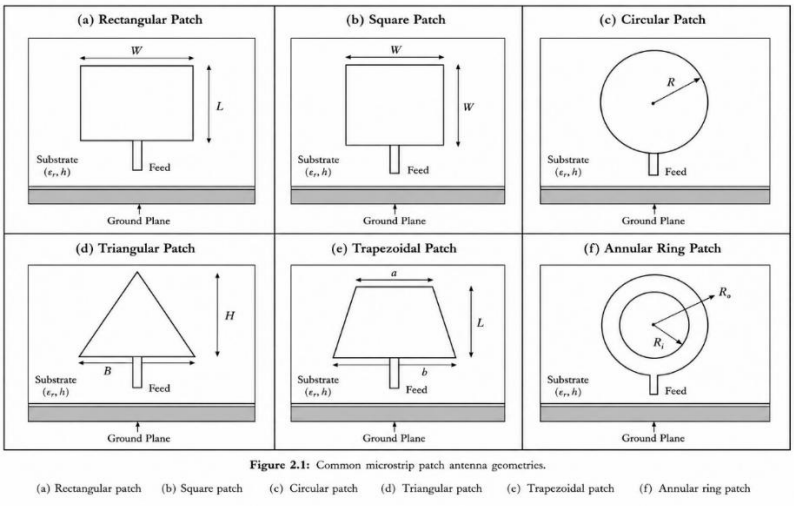


Figure 2: The Six Microstrip Patch Antenna Geometries Investigated in this Study

Rectangular Patch

The width of the rectangular patch was obtained from

$$W = \frac{c}{2f_r}\sqrt{\frac{2}{\varepsilon_r+1}} \quad (1)$$

where c is the velocity of light in free space, f_r is the resonant frequency, and ε_r is the dielectric constant of the substrate. The patch length is obtained as

$$L = L_{eff} - 2\Delta L \quad (2)$$

where L_{eff} is the effective length of the patch, given by

$$L_{eff} = \frac{c}{2f_r\sqrt{\varepsilon_{eff}}} \quad (3)$$

and ε_{eff} is the effective dielectric constant of the substrate, given by

$$\varepsilon_{eff} = \frac{\varepsilon_r+1}{2} + \left[\frac{\varepsilon_r-1}{2}\right](1+12h/W)^{-1/2} \quad (4)$$

ΔL is the extended incremental length of the patch due to fringing effects, given by

$$\Delta L = 0.412h\frac{(\varepsilon_{eff}+0.3)(W/h+0.264)}{(\varepsilon_{eff}-0.258)(W/h+0.8)} \quad (5)$$

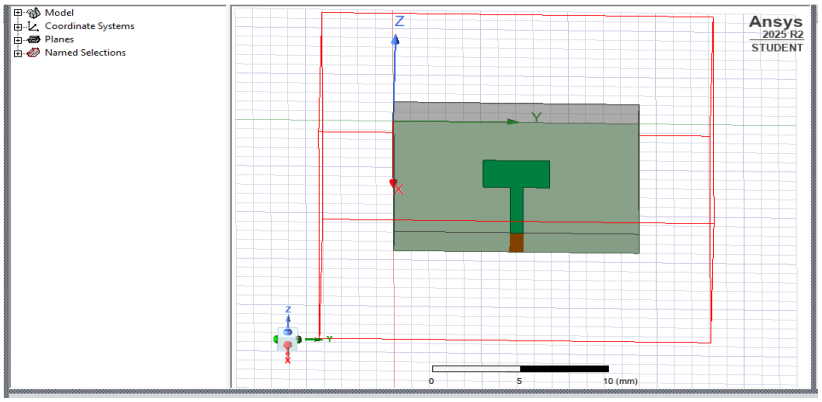


Figure 3: HFSS Model of the Rectangular Microstrip Patch Antenna

Circular Patch

The radius of the circular patch was determined from (Balanis, 2016):

$$a = \frac{F}{\sqrt{1+\frac{2h}{\pi\varepsilon_r F}[ln(\pi F/2h)+1.7726]}} \quad (6)$$

where F is given as

$$F = \frac{8.791\times10^9}{f_r\sqrt{\varepsilon_r}} \quad (7)$$

and h is the substrate thickness (cm), f_r is the resonant frequency (Hz), and Ɛr is the relative permittivity of the substrate. The radius a is obtained in cm.

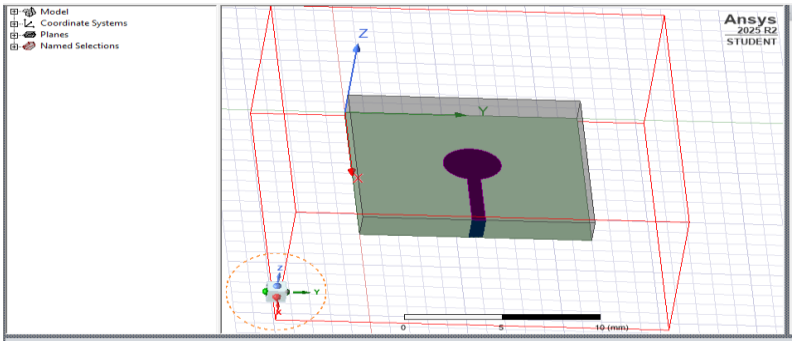


Figure 4: HFSS Model of the Circular Microstrip Patch Antenna

Square Patch

The dimensions of the square patch were obtained using the same effective-length formulation applied to the rectangular patch (Equations 2–5), with the width and length set equal (W = L).

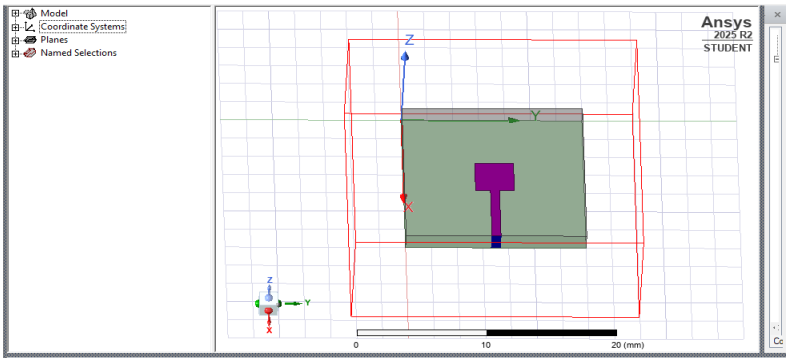


Figure 5. HFSS model of the square microstrip patch Antenna

Triangular Patch

For the equilateral triangular patch, the side length was obtained from

$$a = \frac{2c}{3f_r\sqrt{\varepsilon_r}} \quad (8)$$

where c = 3×10^8 m/s is the velocity of light in free space.

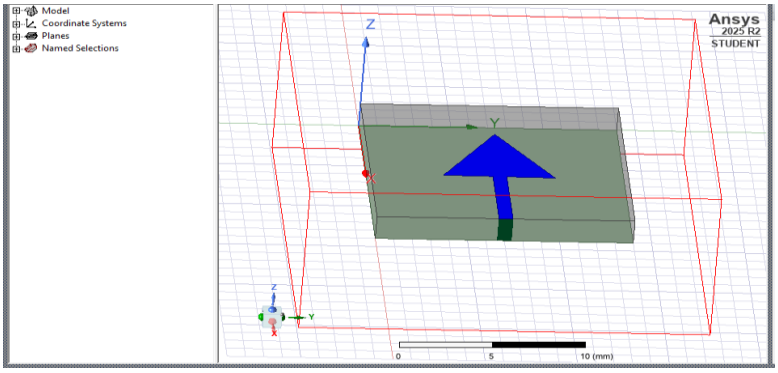


Figure 6: HFSS Model of the Triangular Microstrip Patch Antenna

Annular Ring Patch

The dimensions of the annular ring patch are related to the resonant frequency through

$$\pi(a+b) = \frac{2c}{f_{21}\sqrt{\varepsilon_{eff}}} \quad (9)$$

so that

$$f_{21} = \frac{2c}{\pi(a+b)\sqrt{\varepsilon_{eff}}} \quad (10)$$

where a and b are the outer and inner radii of the ring, respectively.

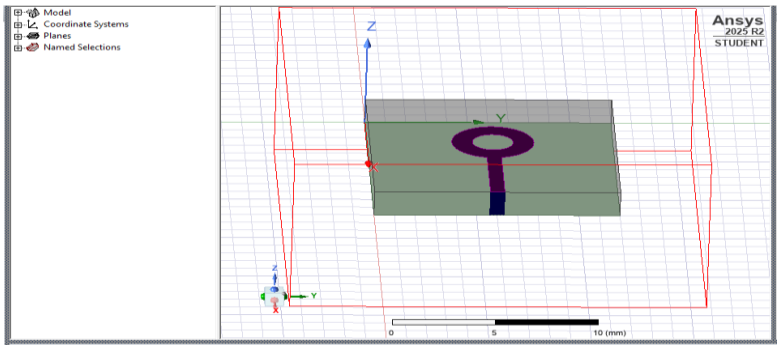


Figure 7: HFSS Model of the Annular Ring Microstrip Patch Antenna

Trapezoidal Patch

The resonant frequency of the trapezoidal patch was approximated using a modified rectangular-patch formulation:

$$f_r = \frac{c}{2L\sqrt{\varepsilon_{eff}}} \quad (11)$$

Since the width of the trapezoidal patch varies along its length, an average width was used:

$$W_{avg} = \frac{W_t+W_b}{2} \quad (12)$$

where W_t and W_b are the top and bottom widths of the patch, respectively.

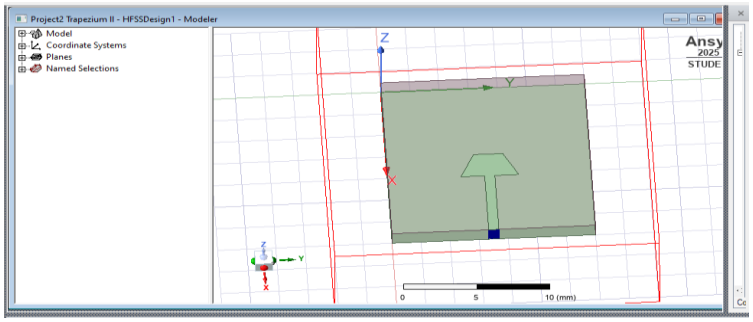


Figure 8: HFSS Model of the Trapezoidal Microstrip Patch Antenna

Design and Simulation Parameters

Table 1 summarizes the substrate properties, simulation software, feed mechanism, and performance parameters common to all six antenna designs.

Table 1: Design and Simulation Parameters

Component / Parameter	Specification
Operating (resonant) frequency	24 GHz
Substrate material	Fire-Resistant Epoxy 4 (FR4)
Substrate relative permittivity (Ɛr)	4.4
Substrate height (h)	1.6 mm
Patch geometries investigated	Rectangular, square, circular, triangular, trapezoidal, annular ring
Simulation software	High Frequency Structure Simulator (HFSS)
Feed mechanism	Microstrip line feed joined directly to the patch edge (no inset feed)
Performance parameters evaluated	Bandwidth, gain, directivity, return loss (S11), voltage standing wave ratio (VSWR)

The physical dimensions of the patch, microstrip feed line, substrate, and ground plane of each of the six simulated antennas are listed in Table 2, together with the frequency sweep range used for each geometry. All designs share the same FR4 substrate thickness (h = 1.6 mm); the substrate and ground plane are 14 mm × 14 mm for all shapes except the circular and annular ring patches, which use 12 mm × 12 mm.

Table 2: Physical Dimensions and Frequency Sweep Range of the Six Simulated Antennas (Dimensions in mm; Sweep Range in GHz)

Patch Shape	Patch Dimensions (mm)	Feed Line, Lf × Wf (mm)	Substrate, Ls × Ws × h (mm)	Ground Plane, Lg × Wg (mm)	Frequency Sweep Range (GHz)
Rectangular	L = 2.8, W = 4.5	3 × 0.75	14 × 14 × 1.6	14 × 14	20 – 36
Triangular	Side length = 3.5 (equilateral)	3 × 0.75	14 × 14 × 1.6	14 × 14	12 – 36
Square	L = W = 3	3 × 0.75	14 × 14 × 1.6	14 × 14	20 – 30
Circular	Radius = 1.5	3 × 0.75	12 × 12 × 1.6	12 × 12	20 – 30
Trapezium	Wt = 2.5 (top), Wb = 4.5 (bottom), L = 3.5	3 × 0.75	14 × 14 × 1.6	14 × 14	12 – 36
Annular Ring	a = 2 (outer radius), b = 0.5 (inner radius)	2.5 × 0.75	12 × 12 × 1.6	12 × 12	20 – 27

RESULTS AND DISCUSSION

To evaluate the performance of the proposed patch geometries, all six antennas were simulated in HFSS at 24 GHz on FR4 substrate, and the resulting bandwidth, gain, directivity, return loss (S11), and voltage standing wave ratio (VSWR) were extracted and compared. The return loss and VSWR were read at the resonant frequency of the S11 minimum nearest the 24 GHz design target, and the bandwidth is the frequency span over which S11 stays below −10 dB, expressed as a percentage of the resonant frequency (BW % = Δf / fr × 100). The simulated resonances occurred at 24.00 GHz (circular and trapezoidal), 24.06 GHz (triangular), 24.28 GHz (rectangular), 24.375 GHz (annular ring), and 24.725 GHz (square), all within about 3% of the 24 GHz target. Such small offsets are expected because closed-form design equations only approximate fringing fields and the effective permittivity, and 24 GHz still lies inside the −10 dB band of each of these antennas. The results obtained for each shape are presented below, followed by a comparative discussion.

Rectangular Patch

The rectangular patch resonated at 24.28 GHz with a return loss of −28.16 dB, corresponding to a VSWR of 1.08. Its −10 dB bandwidth extends from 21.30 GHz to 25.17 GHz (Figure 9), i.e., 3.87 GHz or 15.94% of the resonant frequency. The patch achieved a gain of 6.00 dBi and a directivity of 7.01 dBi, with the three-dimensional patterns shown in Figures 10 and 11. The VSWR plot in Figure 12 shows a minimum of about 1.08 at resonance, indicating very good impedance matching.

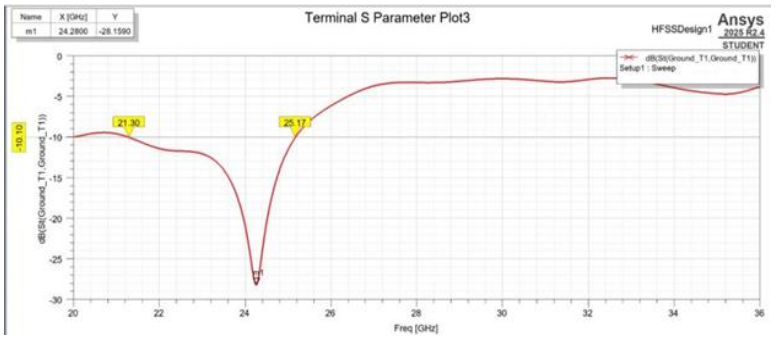


Figure 9: Return Loss (S11) Plot of the Rectangular Patch Showing the -10 dB Bandwidth

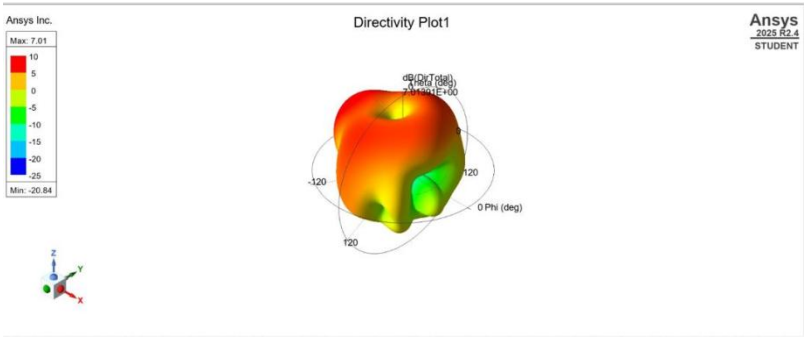


Figure 10: Directivity Radiation Pattern of the Rectangular Patch

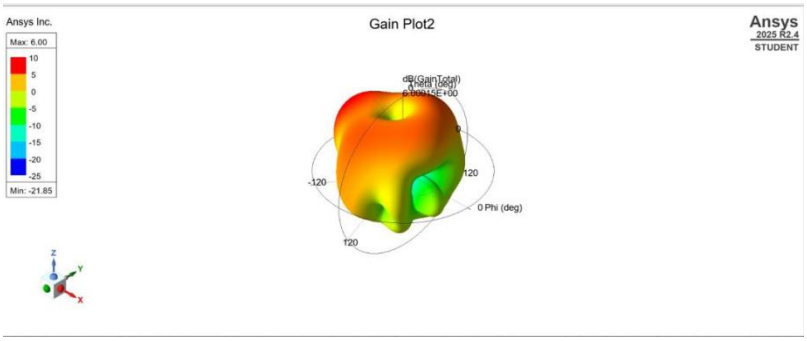


Figure 11: Gain Radiation Pattern of the Rectangular Patch

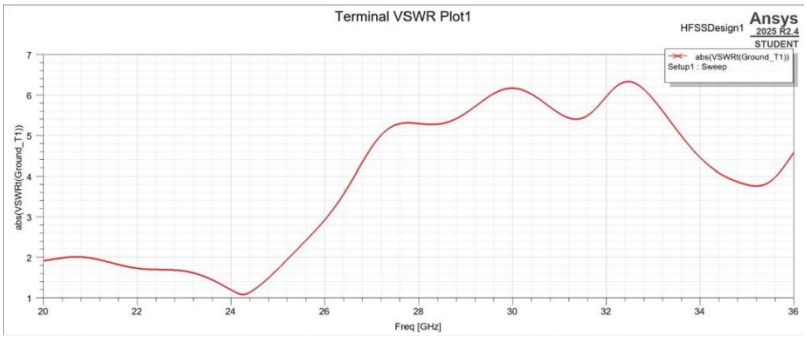


Figure 12: VSWR Plot of the Rectangular Patch

Triangular Patch

The triangular patch resonated at 24.06 GHz and recorded the lowest gain (4.13 dBi) and lowest directivity (5.22 dBi) among the six geometries. Its −10 dB bandwidth spans 22.61–24.50 GHz (1.89 GHz, or 7.86%). Its return loss of −11.02 dB, shown in Figure 13, indicates weaker impedance matching than the rectangular patch, although its VSWR of 1.51 (Figure 16) was still within an acceptable range.

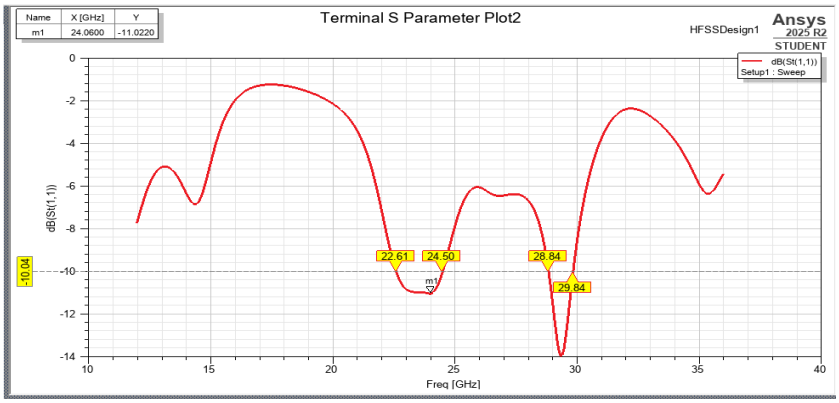


Figure 13: Return Loss (S11) Plot of the Triangular Patch Showing the -10 dB Bandwidth

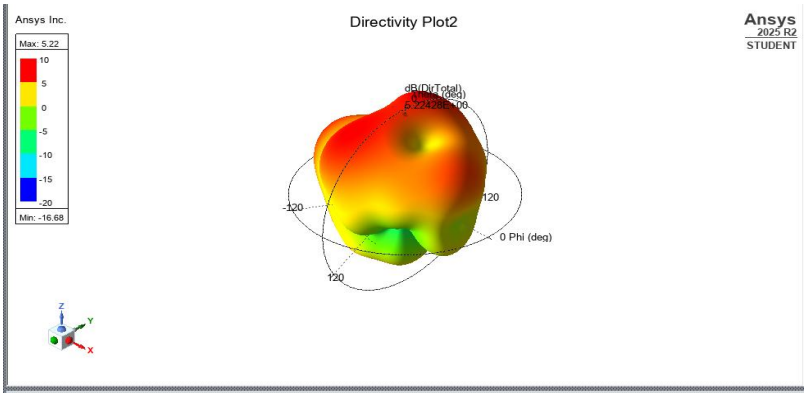


Figure 14: Directivity Radiation Pattern of the Triangular Patch

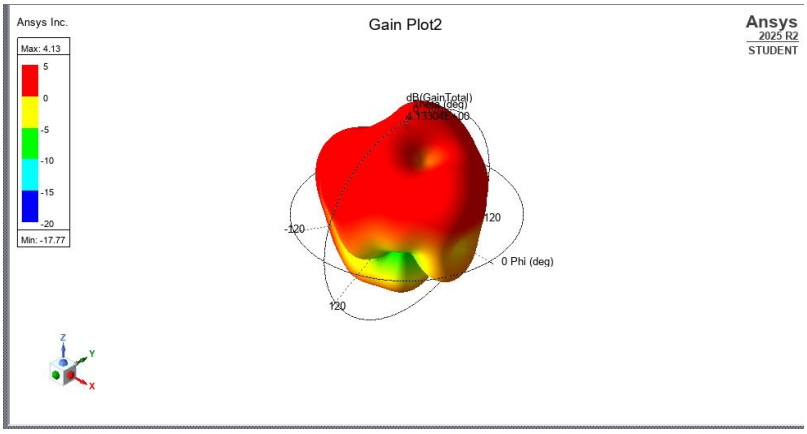


Figure 15: Gain Radiation Pattern of the Triangular Patch

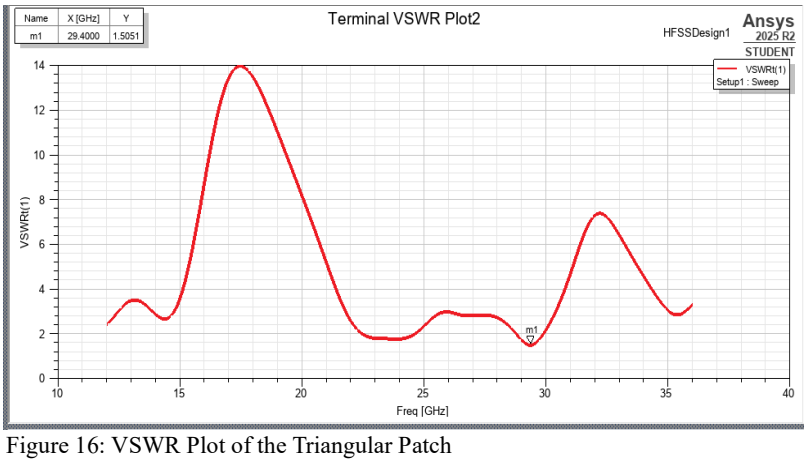


Figure 16: VSWR Plot of the Triangular Patch

Square Patch

The square patch resonated at 24.725 GHz with a return loss of −29.21 dB (Figure 17) and a VSWR of 1.07 (Figure 20). Its −10 dB bandwidth spans 23.73–25.49 GHz, i.e., 1.76 GHz or 7.12% of the resonant frequency. It achieved a directivity of 8.01 dBi and a gain of 7.05 dBi (Figures 18 and 19), showing strong impedance matching at resonance together with high radiation performance.

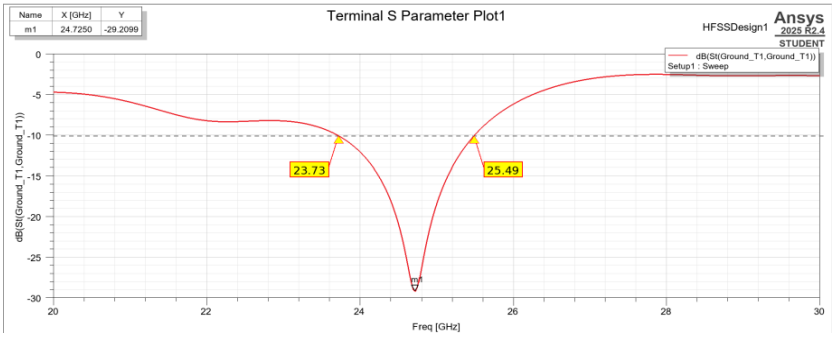


Figure 17: Return Loss (S11) Plot of the Square Patch Showing the -10 dB Bandwidth

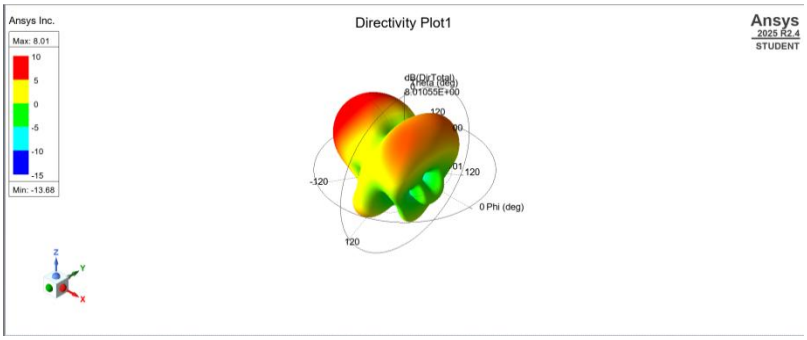


Figure 18: Directivity Radiation Pattern of the Square Patch

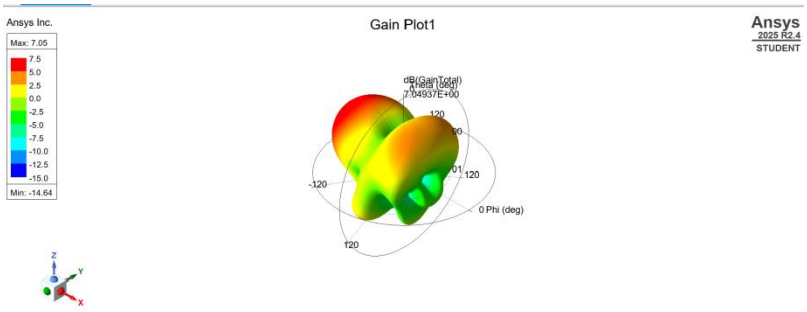


Figure 19: Gain Radiation Pattern of the Square Patch

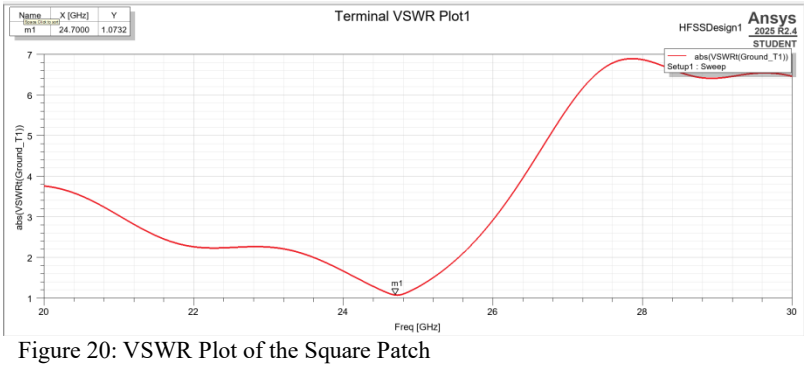


Figure 20: VSWR Plot of the Square Patch

Circular Patch

The circular patch resonated at 24.00 GHz with a return loss of −15.27 dB and a VSWR of 1.42. Its −10 dB bandwidth spans 23.31–24.86 GHz (1.55 GHz, or 6.46%), and it achieved a gain of 6.11 dBi and a directivity of 6.78 dBi. As shown in Figures 21–24, the S11 curve has a well-defined resonance at the design frequency; a second, shallower resonance of about −13.8 dB also appears near 28 GHz, outside the band of interest.

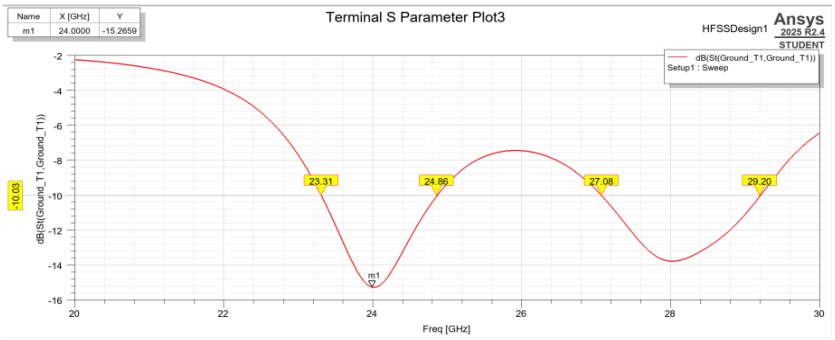


Figure 21: Return Loss (S11) Plot of the Circular Patch Showing the -10 dB Bandwidth

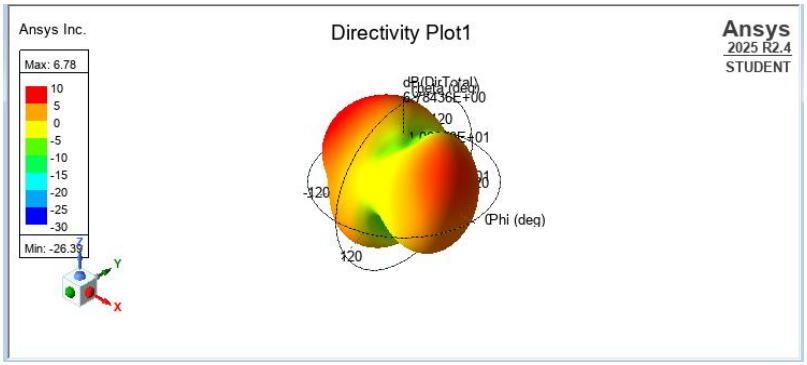


Figure 22: Directivity Radiation Pattern of the Circular Patch

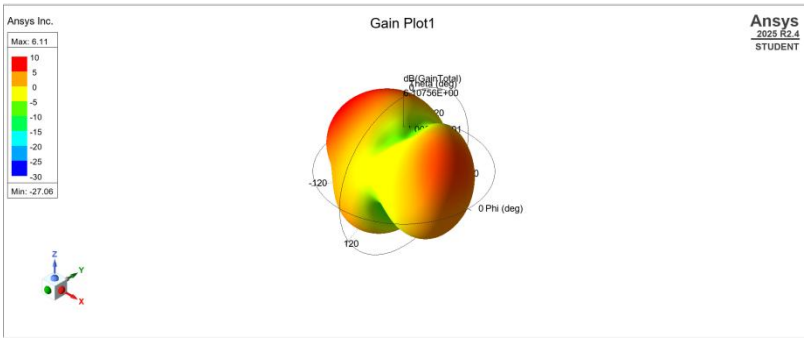


Figure 23: Gain Radiation Pattern of the Circular Patch

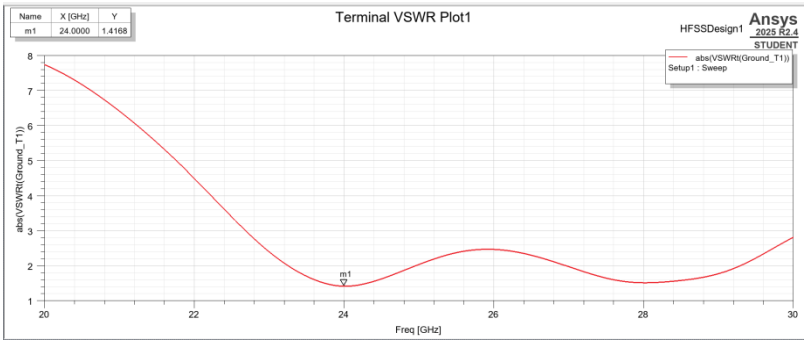


Figure 24: VSWR Plot of the Circular Patch

Trapezoidal Patch

The trapezoidal patch resonated at 24.00 GHz with a return loss of −13.85 dB (Figure 25) and a VSWR of 1.51 (Figure 28). Its −10 dB bandwidth spans 23.50–24.50 GHz, i.e., 1.00 GHz or 4.17% of the resonant frequency, the narrowest of the six shapes. It achieved a gain of 6.13 dBi and a directivity of 7.07 dBi (Figures 26 and 27).

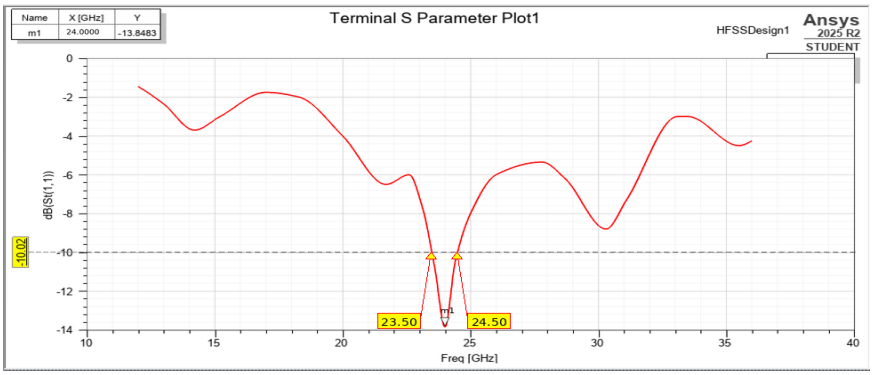


Figure 25: Return Loss (S11) Plot of the Trapezoidal Patch Showing the -10 dB Bandwidth

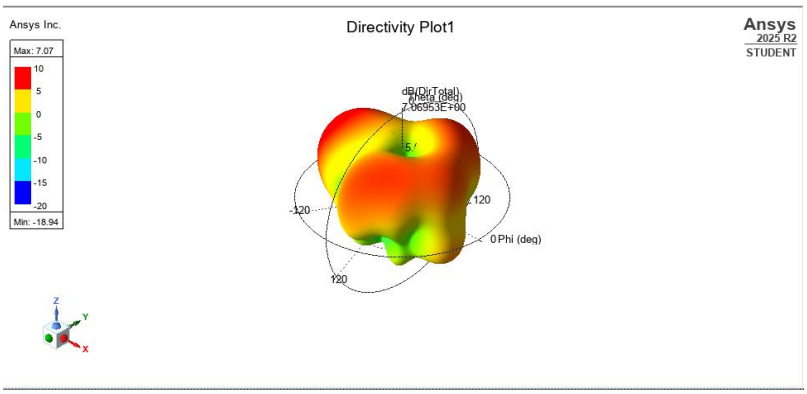


Figure 26: Directivity Radiation Pattern of the Trapezoidal Patch

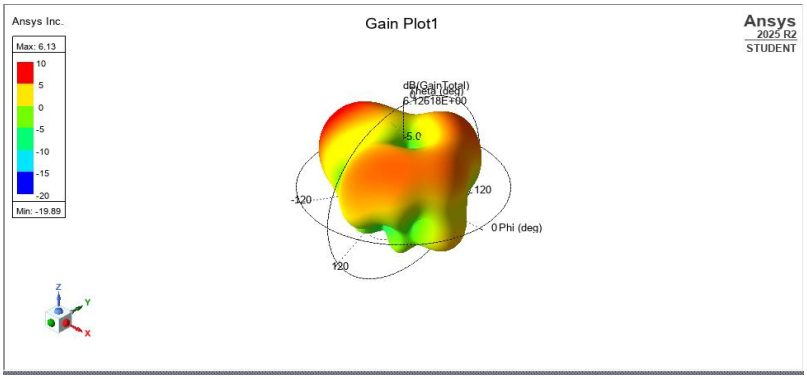


Figure 27: Gain Radiation Pattern of the Trapezoidal Patch

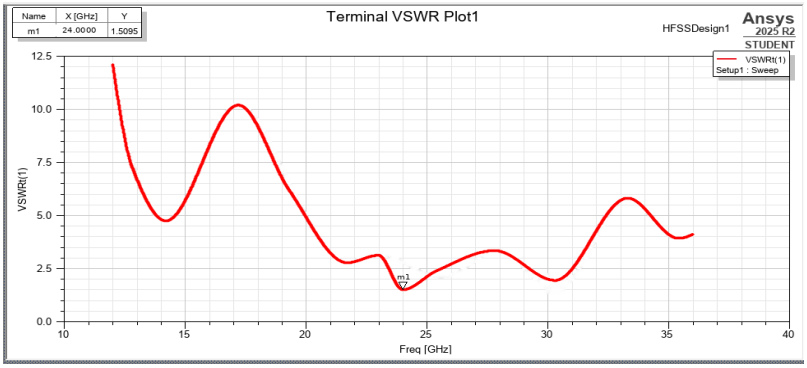


Figure 28: VSWR Plot of the Trapezoidal Patch

Annular Ring Patch

The annular ring patch resonated at 24.375 GHz with a return loss of −14.51 dB (Figure 29) and a VSWR of 1.46 (Figure 32). Its −10 dB bandwidth spans 23.64–25.71 GHz, i.e., 2.07 GHz or 8.49% of the resonant frequency. It also achieved a gain of 7.18 dBi and a directivity of 8.01 dBi (Figures 30 and 31), showing that good impedance matching at resonance was obtained together with strong radiation performance.

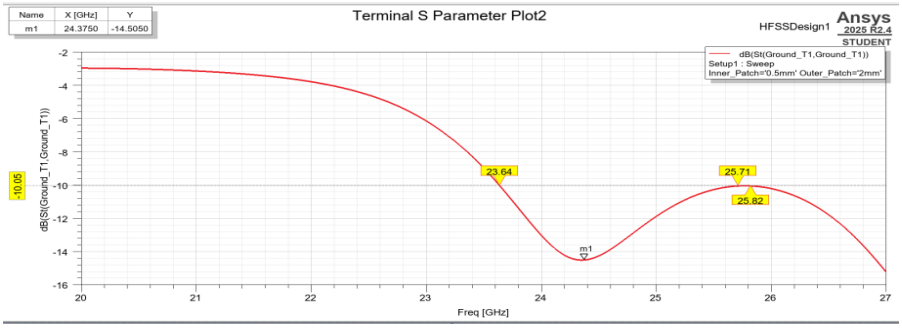


Figure 29: Return Loss (S11) Plot of the Annular Ring Patch Showing the -10 dB Bandwidth

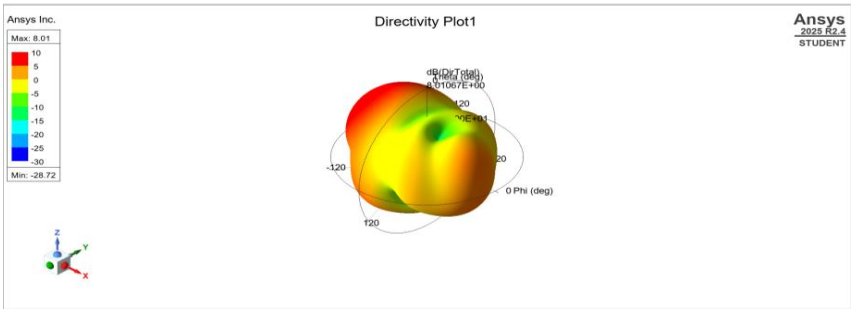


Figure 30: Directivity Radiation Pattern of the Annular Ring Patch

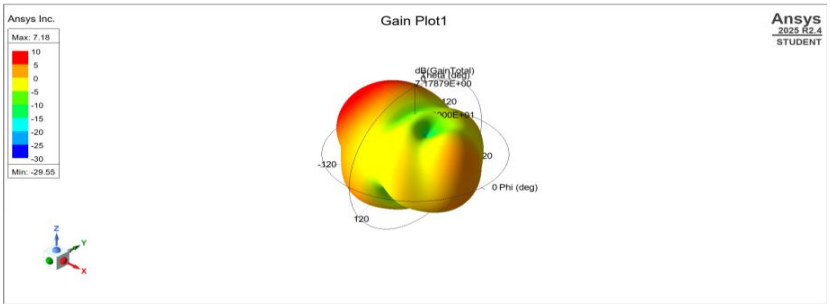


Figure 31: Gain Radiation Pattern of the Annular Ring Patch

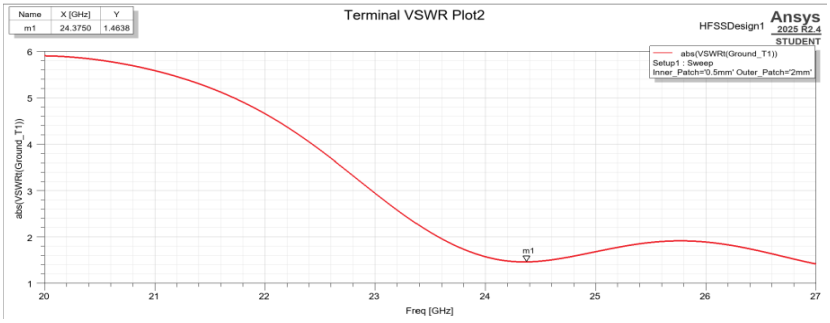


Figure 32: VSWR Plot of the Annular Ring Patch

RESULTS AND DISCUSSION

Summary of Results

Table 3: Summary of Simulated Performance Across the Six Patch Geometries

Patch Shape	Resonant Frequency (GHz)	Bandwidth, −10 dB (GHz / %)	Gain (dBi)	Return Loss (dB)	Directivity (dBi)	VSWR
Rectangular	24.28	3.87 / 15.94	6.00	-28.1590	7.01	1.0814
Triangular	24.06	1.89 / 7.86	4.13	-11.0220	5.22	1.5051
Square	24.73	1.76 / 7.12	7.05	-29.2099	8.01	1.0732
Circular	24.00	1.55 / 6.46	6.11	-15.2659	6.78	1.4168
Trapezium	24.00	1.00 / 4.17	6.13	-13.8483	7.07	1.5095
Annular Ring	24.38	2.07 / 8.49	7.18	-14.5050	8.01	1.4638

Discussion

The simulated performance of the six geometries is summarized in Table 3, and Table 4 places the present results alongside related studies. The results confirm that patch geometry has a measurable effect on every performance parameter evaluated. All six antennas resonated close to the 24 GHz design target (24.00–24.725 GHz). The rectangular patch achieved by far the widest bandwidth (15.94%) together with a deep return loss (−28.16 dB) and a very low VSWR (1.08), making it the most suitable geometry where bandwidth-limited operation — the central problem motivating this study — is the primary design concern. The square patch delivered the deepest return loss (−29.21 dB) and the lowest VSWR (1.07) with a high gain of 7.05 dBi, although its bandwidth (7.12%) was less than half that of the rectangular patch. The annular ring patch recorded the highest gain (7.18 dBi) and a directivity of 8.01 dBi (equal to the square patch) while keeping a good match (VSWR 1.46) and the second-widest bandwidth (8.49%), suggesting that its wider radiating aperture and ring-shaped current distribution improve radiation efficiency. The circular patch gave a balanced but unremarkable performance (6.46% bandwidth, 6.11 dBi gain, VSWR 1.42). The trapezoidal patch achieved similar gain (6.13 dBi) and directivity (7.07 dBi) but had the narrowest bandwidth (4.17%) and a comparatively high VSWR (1.51). The triangular patch underperformed in gain (4.13 dBi), directivity (5.22 dBi), and return loss (−11.02 dB), which is attributable to its smaller effective radiating area compared to the other geometries at the same resonant frequency. Overall, no single geometry dominates every performance metric; rather, the rectangular shape is best suited to bandwidth-critical 5G applications, the square shape to applications that demand the best impedance match, and the annular ring to applications where gain and directivity are prioritized.

Table 4: Comparison with Related Studies

Reference	Frequency	Substrate	Shapes Compared	Gain (dBi)	Bandwidth	Platform
Gemeda et al. (2021)	28 GHz	FR-4	Rectangular only	7.587	1.046 GHz	CST
Kiran et al. (2018)	28.3 / 50.3 GHz	Rogers RT 5880	Rectangular only	2.6	Not reported	CST
Colaco & Lohani (2020)	27 GHz	RT/Duroid	Circular, Rectangular, Square	Not reported	Rectangular best	HFSS
Proposed work	24 GHz	FR4	Rectangular, Circular, Triangular, Square, Trapezium, Annular ring	4.13 - 7.18	4.17 - 15.94%	HFSS

CONCLUSION

This study presented a comparative analysis of six microstrip patch antenna geometries — rectangular, square, circular, triangular, trapezoidal, and annular ring — designed and simulated at 24 GHz on an FR4 substrate in HFSS, with performance evaluated in terms of bandwidth, gain, directivity, return loss (S11), and voltage standing wave ratio (VSWR). The results confirm that patch geometry has a measurable and consistent effect on every performance parameter considered, demonstrating that shape selection is a critical design variable rather than an incidental one for microstrip antennas operating at millimeter-wave frequencies. The rectangular patch achieved the widest bandwidth (15.94%) together with a deep return loss (−28.16 dB) and a very low VSWR (1.08), making it the most suitable geometry for bandwidth-limited 5G applications — the central problem motivating this study. The square patch achieved the deepest return loss (−29.21 dB) and the lowest VSWR (1.07) alongside a high gain of 7.05 dBi, while the annular ring patch delivered the highest gain (7.18 dBi) and a directivity of 8.01 dBi. The circular and trapezoidal patches offered moderate gain (about 6.1 dBi), but the trapezoidal patch had the narrowest bandwidth (4.17%). The triangular patch consistently underperformed in gain, directivity, and return loss, attributable to its smaller effective radiating area relative to the other geometries at the same resonant frequency.

Taken together, these findings show that no single geometry dominates every performance metric. The rectangular shape offers the widest bandwidth, the square shape the best impedance matching, and the annular ring the highest gain and directivity. These results provide practical, evidence-based guidance for antenna designers selecting a patch geometry for compact, high-performing 5G and future millimeter-wave wireless communication systems, and they underscore the value of evaluating candidate geometries under identical design, substrate, and simulation conditions rather than in isolation.

Future work should extend this comparison to low-loss and high-frequency substrates (e.g., Rogers RT/Duroid), evaluate array configurations of the best-performing geometries, and validate the simulated results through fabrication and measurement to confirm their practical viability for 5G mm-wave deployment.

REFERENCES

Agiwal, M., Roy, A., & Saxena, N. (2016). Next generation 5G wireless networks: A comprehensive survey. *IEEE Communications Surveys & Tutorials, 18*(3), 1617–1655. https://doi.org/10.1109/COMST.2016.2532458

Andrews, J. G., Buzzi, S., Choi, W., Hanly, S. V., Lozano, A., Soong, A. C. K., & Zhang, J. C. (2014). What will 5G be? *IEEE Journal on Selected Areas in Communications, 32*(6), 1065–1082. https://doi.org/10.1109/JSAC.2014.2328098

Balanis, C. A. (2016). *Antenna theory: Analysis and design* (4th ed.). Wiley. https://www.wiley.com/en-us/antenna-theory-analysis-and-design-4th-edition-p-9781118642061

Bansal, A., & Gupta, R. (2020). A review on microstrip patch antenna and feeding techniques. *International Journal of Information Technology, 12*(1), 149–154. https://doi.org/10.1007/s41870-018-0121-4

Colaco, J., & Lohani, R. B. (2020). Design and implementation of microstrip circular patch antenna for 5G applications. In *2020 International Conference on Electrical, Communication, and Computer Engineering (ICECCE)* (pp. 1–4). IEEE. https://doi.org/10.1109/ICECCE49384.2020.9179263

Gemeda, M. T., Fante, K. A., Goshu, H. L., & Goshu, A. L. (2021). Design and analysis of a 28 GHz microstrip patch antenna for 5G communication systems. *International Research Journal of Engineering and Technology, 8*(2), 881–886. https://repository.ju.edu.et/handle/123456789/6084

Kiran, T., Mounisha, N., Mythily, C., Akhil, D., & Kumar, T. V. B. P. (2018). Design of microstrip patch antenna for 5G applications. *IOSR Journal of Electronics and Communication Engineering, 13*(1), 14–17. https://doi.org/10.9790/2834-1301011417

Kiruthika, R., &Shanmuganantham, T. (2016). Comparison of different shapes in microstrip patch antenna for X-band applications. In *2016 International Conference on Emerging Technological Trends (ICETT)* (pp. 1–6). IEEE. https://doi.org/10.1109/ICETT.2016.7873722

Lan, N. T. M. (2023). Evolution of wireless technology: From 1G to 5G. *Asian Journal of Applied Science and Technology, 7*(4), 68–73. https://doi.org/10.38177/ajast.2023.7408

Pandey, P., Agrawal, N., & Agrawal, A. (2019). A survey on performance enhancement techniques for microstrip patch antenna. *International Journal of Research and Analytical Reviews, 6*(1), 669–676. https://ijrar.org/papers/IJRAR19J1220.pdf

Reviewer Corrections — Highlighting Key

Yellow highlighting identifies text in the supplied corrected manuscript that addresses points raised in the reviewer report. It does not prove that the text was newly added: the original pre-revision manuscript was not supplied for a tracked comparison.

Physical Dimensions

Addressed: Table 2 lists patch, feed, substrate and ground-plane dimensions for all six geometries.

HFSS Simulation Details

Addressed in the Design Procedure: radiation boundary, adaptive meshing (maximum 20 passes), delta S (0.02), and geometry-specific sweep ranges.

Feed-Matching Description

Addressed: direct edge-connected microstrip feed, without inset or matching section. The report mentions a 50 Ω feed; the corrected text does not explicitly confirm its impedance.

Frequency Discrepancy

Partially addressed in text: revised resonant frequencies and a definition of the −10 dB band are supplied. Independent confirmation against the original HFSS output and figure markers is still required.

Annular Ring Bandwidth

Addressed: the narrative reports 2.07 GHz (8.49%). Note that the reviewer cited an earlier 1.23% value, which cannot be reconciled without the original manuscript/data.

Missing Reference DOI/URL

Addressed with URLs for Gemeda et al. (2021) and Pandey et al. (2019). These are URL alternatives, not verified DOIs.

©2026 This is an Open Access article distributed under the terms of the Creative Commons Attribution 4.0 International license viewed via https://creativecommons.org/licenses/by/4.0/ which permits unrestricted use, distribution, and reproduction in any medium, provided the original work is cited appropriately.